Electronic Supplementary Information (ESI)
In situ TEM analysis of resistive switching in manganite based thin–film heterostructures.

Jonas Norpoth, Stephanie Mildner, Malte Scherff, Jörg Hoffmann, and Christian Jooss*

Received Xth XXXXXXXXXX 20XX, Accepted Xth XXXXXXXXX 20XX
First published on the web Xth XXXXXXXXXX 200X
DOI: 10.1039/b000000x

1 ESI text

1.1 EFTEM and EELS data analysis

EFTEM imaging has been performed in order to determine elemental maps of TEM–samples before and after electrical stimulus. We adopted the 3–window method following the guidelines provided by Kothleitner and Hofer.[1] The oxygen elemental maps are quantified as $N = I_{\mathrm{k}}/(I_{\mathrm{low}} \cdot \sigma_{\mathrm{k}} \cdot \Lambda)$. Therein, I_{k} represents the O K 3–window map, I_{low} the corresponding low–loss image including the zero–loss peak and σ_{k} the partial inelastic scattering cross–section calculated with Egerton's hydrogenic model.[2] The absolute thickness map Λ is calculated by multiplication of the measured relative thickness map with the inelastic mean free path λ, which has been parameterized by Malis *et al.* for TEM applications.[3] We use a uniform value of $\lambda = 107.5$ nm as the average of $\lambda^{\mathrm{PCMO}} = 110$ nm and $\lambda^{\mathrm{STNO}} = 105$ nm. The quantification accuracy is estimated to be not better than 20% given the errors in the parameterization of λ as well as by the ELNES contribution to the O K signal, which is not included in the atomic model used for the calculation of σ_{k}. The main purpose of this scheme is to eliminate detrimental contributions of diffraction contrast and sample thickness inhomogenities from the elemental maps.

STEM/EELS line scans across the interfaces between PCMO and the electrodes provide elemental distributions with high spatial resolution as well as access to the local electronic properties by the ELNES of core–loss edges. We determined relative elemental compositions using the built–in quantification routine of Gatan DM software. ESI–Fig. 1 demonstrates the analysis of the O K ELNES, which was applied to determine the position of the feature K_1.

1.2 PCMO microstructure

X–ray diffraction and SAD reveal epitaxial growth of the PCMO films in <001> direction (notation in space group $Pbnm$). As displayed in ESI–Fig. 2, there are two types of epitaxial twin variants with diameters on the order of 100 nm and in–plane relations PCMO<100> ‖ STNO<110> or PCMO<010> ‖ STNO<110>, respectively ($Pm\bar{3}m$ notation for STNO). A minor portion of misoriented grains is grown on top of incoherent precipitates with diameters on the order of $1-10$ nm at the interface to the STNO substrate. The precipitates are $\mathrm{Mn_2O_3}$ nanoparticles as evident in a measured elemental Mn/O ratio of 2/3 as well as an increased Mn $\mathrm{L_2}$–$\mathrm{L_3}$ peak separation of 11 eV (*cf.* reference[4]), see ESI–Fig. 2(b).

References

1 G. Kothleitner and F. Hofer, *Micron*, 1998, **29**, 349.
2 R. F. Egerton, *Ultramicroscopy*, 1979, **4**, 169.
3 T. Malis, S. C. Cheng and R. F. Egerton, *Journal of Electron Microscopy Technique*, 1988, **8**, 193.
4 J. H. Rask, B. A. Miner and P. R. Buseck, *Ultramicroscopy*, 1987, **21**, 321.

2 ESI figures

Institut für Materialphysik, Universität Göttingen, Friedrich–Hund–Platz 1, 37077 Göttingen, Germany.
* E-mail: jooss@material.physik.uni-goettingen.de

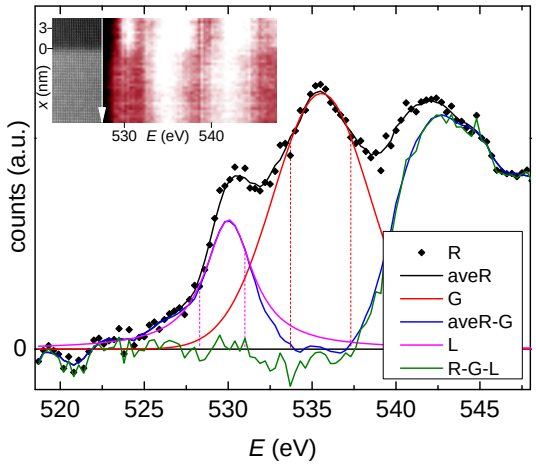

Fig. 1 O K ELNES analysis to determine the position of the K_1 peak. The raw data of an individual spectrum ("R") is smoothed with a weighted, 5–point moving average filter ("aveR"). A Gaussian is fitted to the K_2 peak ("G") and subtracted from the smoothed data ("aveR–G"). Finally, a Lorentzian is fitted to the residual K_1 peak ("L"). The dashed, vertical lines indicate the respective windows for the fittings. Inset: Z–contrast ADF micrograph of the pn junction and corresponding O K ELNES in a line scan along the arrow from STNO to PCMO.

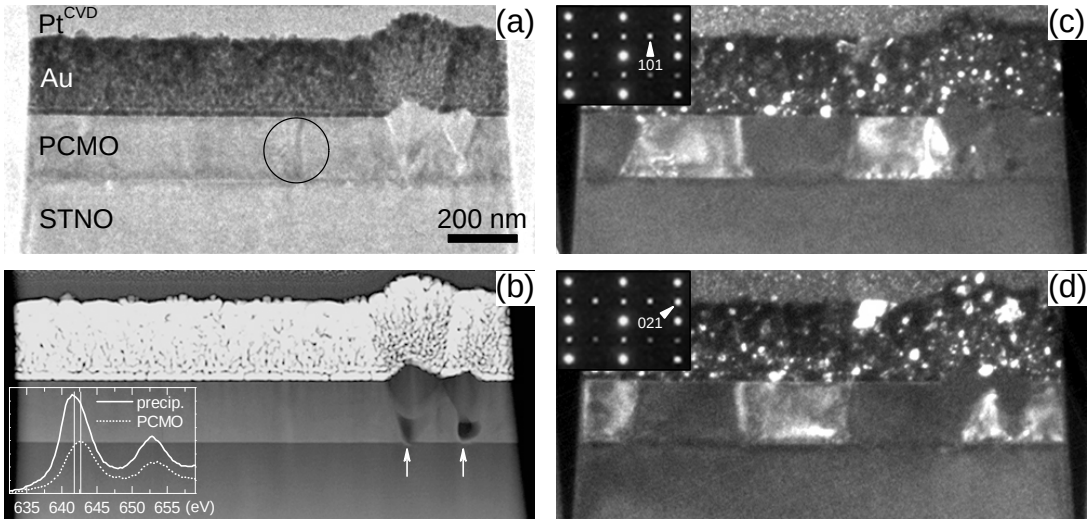

Fig. 2 Microstructure of a TEM–sample with two precipitates. **(a)** BF overview. **(b)** Z–contrast ADF. The arrows mark precipitates in the PCMO film at the interface to the STNO. Inset: Mn $L_{2,3}$ ELNES point–spectra from precipitate and PCMO film. **(c)–(d)** DF twin imaging with the spots marked in the inset SAD patterns from the area indicated by the circle in (a).

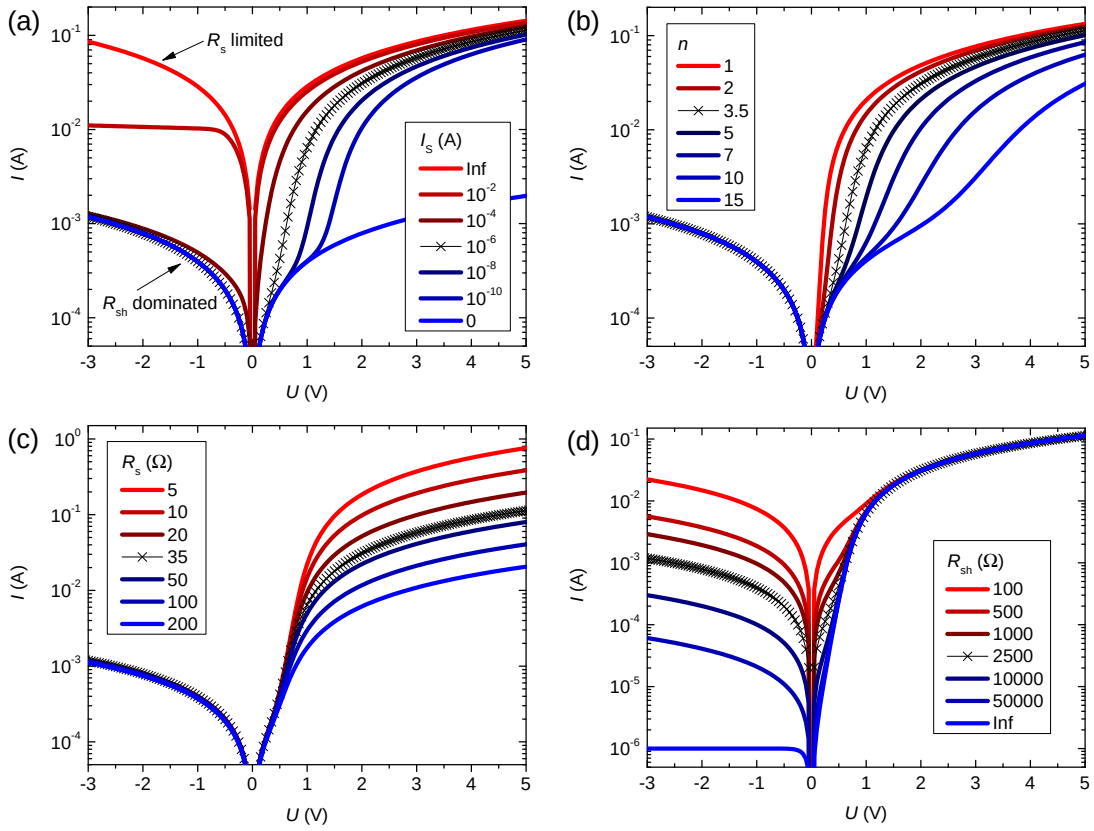

Fig. 3 Equivalent–circuit model: influence of the individual components on the current–voltage characteristics. The reference set of parameters ($I_{\mathrm{S}} = 10^{-6}$ A, $n = 3.5$, $R_{\mathrm{s}} = 35\ \Omega$, $R_{\mathrm{sh}} = 2500\ \Omega$) corresponds to a typical 7–μm pad–sample (crosses). Variation of **(a)** I_{S}, **(b)** n, **(c)** R_{s} and **(d)** R_{sh} with the respectively other parameters fixed to their reference values.

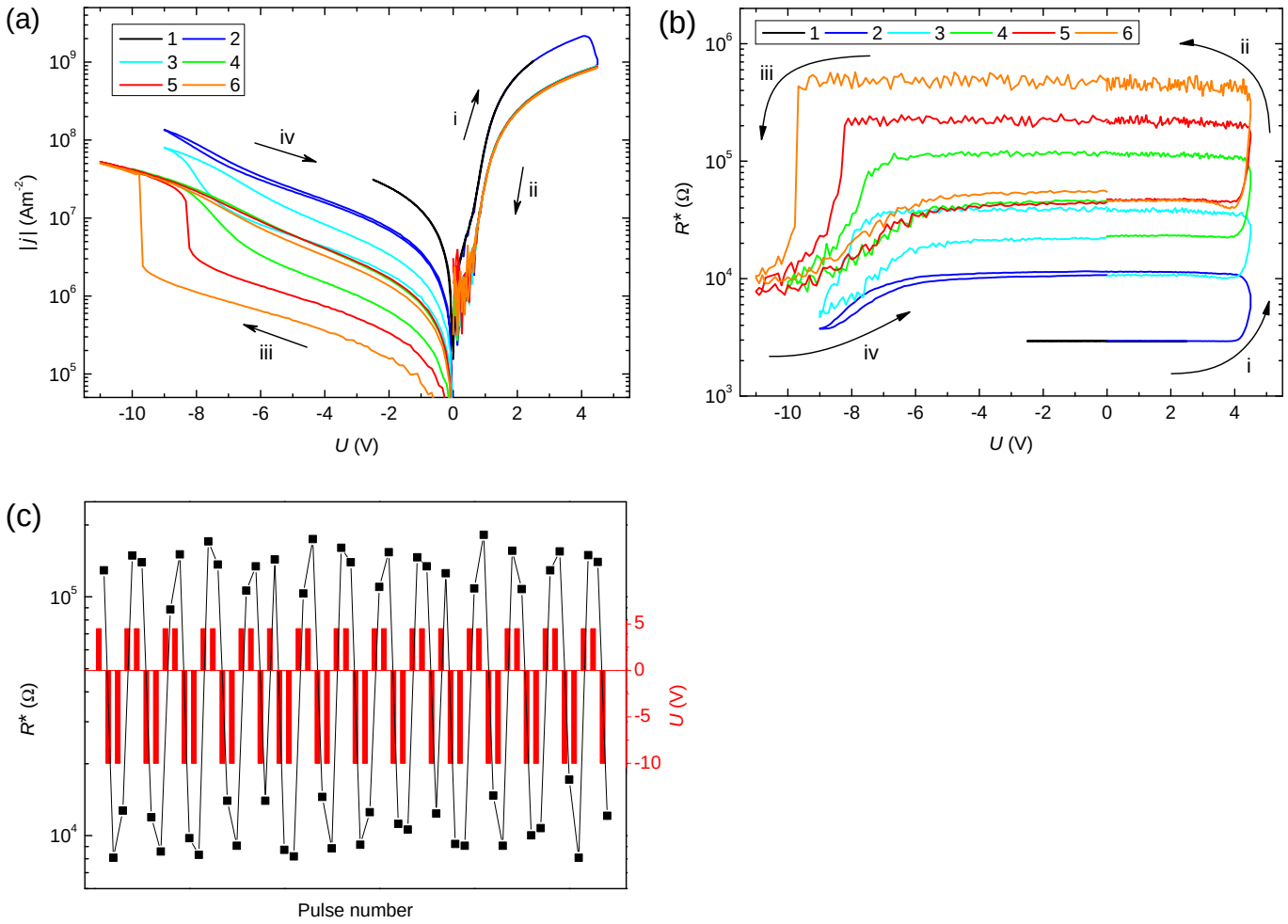

Fig. 4 Electric–pulse induced resistive switching in a pad–sample. **(a)** Successive current–voltage curves, each revolved as indicated by the labelled arrows. According to the equivalent–circuit analysis, the model parameters in the initial(final) state are $j_{\rm S} = 1.5(0.55) \times 10^4$ Am^{-2}, $n = 4(4)$, $R_{\rm s} = 46(137)$ Ω and $R_{\rm sh} = 2800(\sim 4 \times 10^4)$ Ω, where the final value of $R_{\rm sh}$ corresponds to stage `iii` on branch `6` before the reverse switch. **(b)** Resistance in intermediate pulses of 0.05 V forward bias between the incremental pulses in (a). **(c)** Write/read/erase protocol after branch `6`. Resistance in intermediate pulses of 0.05 V forward bias (black symbols) between high-bias pulses (red columns).

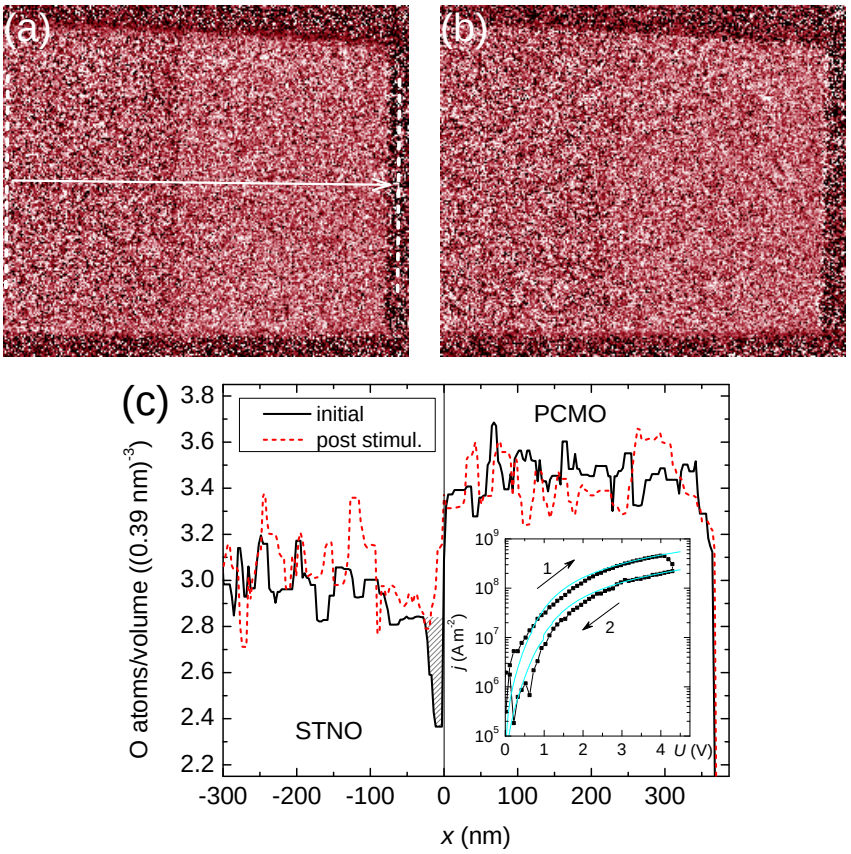

Fig. 5 False–color maps of oxygen atomic volume density from EFTEM **(a)** before and **(b)** after electric–pulse induced HRS formation. **(c)** Averaged line profiles from areas as indicated in (a), $x = 0$ corresponds to the position of the junction. The profiles are additionally smoothed by a median filter of 15–nm width. Inset: *in situ* current–voltage curve (symbols) and corresponding fits (lines); the map in (b) was acquired after this stimulus. Fit parameters on branch $1(2)$ are $j_{\mathrm{S}} = 5(1) \times 10^5$ Am^{-2}, $n = 7(7)$, $R_{\mathrm{s}} = 1.4(3.2) \times 10^5\ \Omega$ and $R_{\mathrm{sh}} \approx 7(7) \times 10^7\ \Omega$.

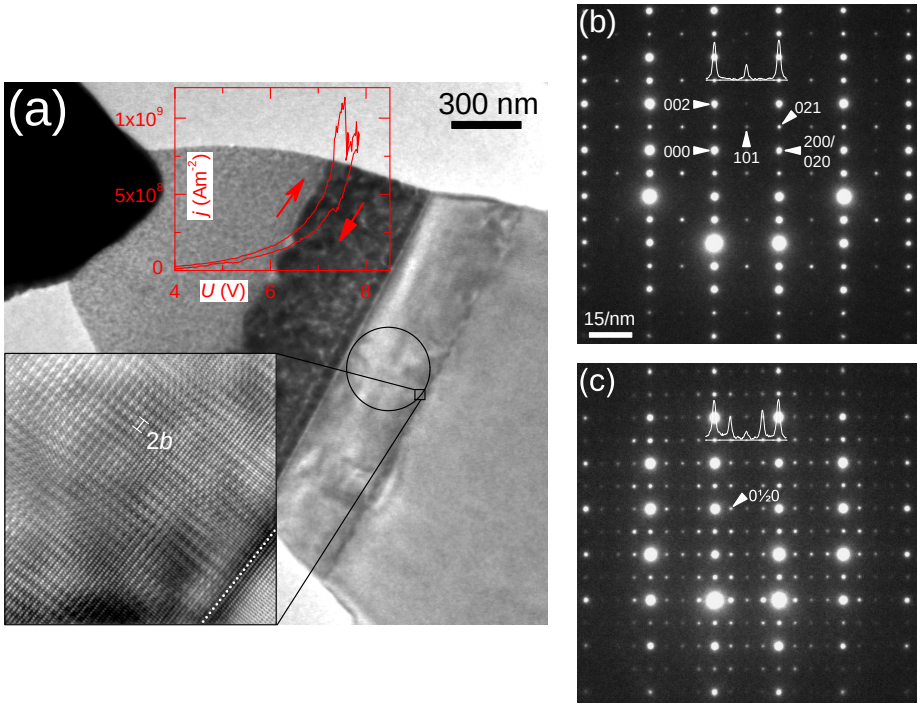

Fig. 6 Superstructure formation in PCMO during resistive switching. **(a)** BF overview of a TEM–sample in contact with the nano–tip. Top inset: corresponding *in situ* current–voltage curve with HRS formation. Note, that a continuous voltage sweep mode was applied in this experiment. Bottom inset: high–resolution BF micrograph of the $2b$ superstructure induced during the HRS formation. The image is Fourier–filtered in order to better visualize the lattice modulation along the b–direction. The dotted line indicates the interface to the substrate. SAD patterns of the PCMO film (projected aperture position marked by the circle in (a)) **(b)** before and **(c)** after the HRS formation.

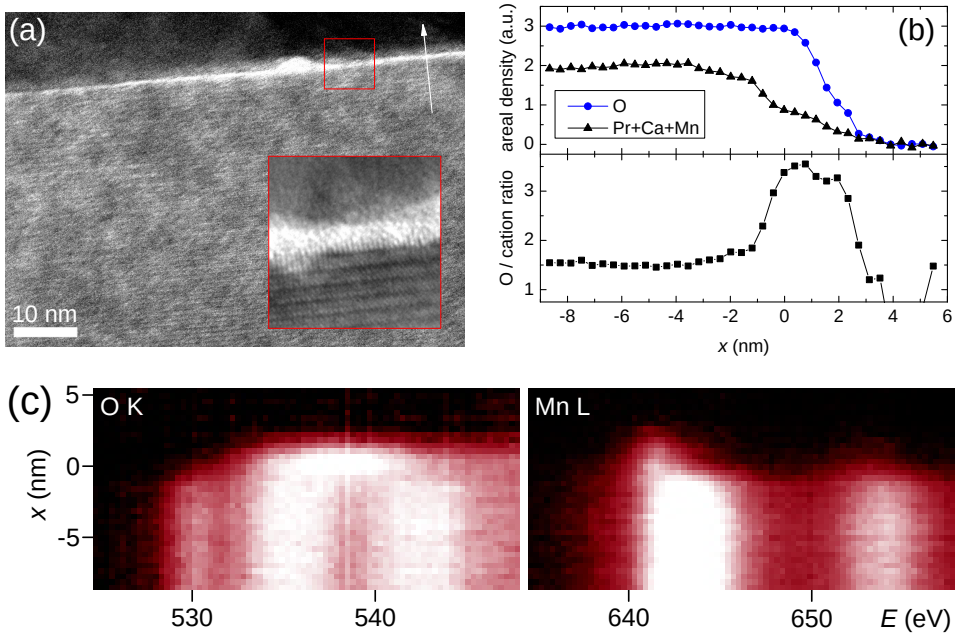

Fig. 7 Interface between PCMO and Au top electrode. **(a)** BF micrograph. Inset: high–resolution BF of the area marked by the red box (8×8 nm^2). **(b)** Elemental composition determined from a STEM/EELS line scan along the arrow in (a). Areal densities of oxygen and all cations summed up (top panel) and their ratio (bottom). **(c)** O K and Mn $L_{2,3}$ ELNES along the arrow in (a).